Materials Today Advances 5 (2020) 100023

Contents lists available at ScienceDirect

Materials Today Advances

journal homepage: www.journals.elsevier.com/materials-today-advances/

Advanced biocomposites of poly(glycerol sebacate) and β-tricalcium phosphate by *in situ* microwave synthesis for bioapplication

C.C. Lau [a], M. Al Qaysi [b], N. Owji [b], M.K. Bayazit [a, c], J. Xie [a], J.C. Knowles [b, d, e, f], J. Tang [a, *]

[a] Department of Chemical Engineering, University College London, Torrington Place, London WC1E 7JE, UK
[b] Division of Biomaterials and Tissue Engineering, UCL Eastman Dental Institute, 256 Gray's Inn Road, London, WC1X 8LD, UK
[c] SUNUM Nanotechnology Research and Application Centre, Sabanci University, 34956, Tuzla, Istanbul, Turkey
[d] The Discoveries Centre for Regenerative and Precision Medicine, UCL Campus, London, UK
[e] Department of Nanobiomedical Science and BK21 Plus NBM Global Research Centre for Regenerative Medicine and Institute of Tissue Regeneration Engineering (ITREN), Dankook University, Republic of Korea
[f] UCL Eastman-Korea Dental Medicine Innovation Centre, Dankook University, Cheonan 31114, Republic of Korea

ARTICLE INFO

Article history:
Received 19 February 2019
Received in revised form
29 August 2019
Accepted 25 September 2019
Available online xxx

Keywords:
Composite
Hydrophilicity
Degree of cross-linking
Degradation rate
Cell proliferation

ABSTRACT

Biodegradable poly(glycerol sebacate) [PGS] has gained substantial attention in the soft tissue engineering field over the past few years, but its application is limited because its fast degradation rate causes an acidic environment which can adversely affect cell viability and eventually tissue growth. β-tricalcium phosphate (β-TCP) is an ideal biocompatible candidate to mitigate these drawbacks of PGS. This work for the first time rationalizes a biocomposite composed of PGS and β-TCP prepared by a fast and well-controlled microwave approach. As expected, the presence of β-TCP particles (i) improves the degree of cross-linking of PGS, thus decreasing the sol content by ca. 66%, (ii) enhances its hydrophilicity with much lower contact angle, (iii) reduces the degradation rate by a factor of two and (iv) increases the swelling effect of the biocomposite by ca. 10%. Furthermore both PGS/β-TCP150 and PGS/β-TCP180 biocomposites demonstrate significant difference in cell viability form the single PGS materials, which is more than 65% higher in cell growth in one day proliferation, demonstrating an advanced biomaterial embodying both advantages of PGS polymer and β-TCP bioceramics.

1. Introduction

Substantial efforts have been put into developing the synthetic biopolymers mimicking the physical and molecular properties of natural tissues. Synthetic biopolymers can be categorized into biodegradable and non-biodegradable polymers. For instance, polyetheretherketone is one of the most popular non-degradable biopolymers and has been preferred for the applications requiring high resistance to both thermal degradation and biodegradation [1,2]. The biodegradable polymeric biomaterials, dominated by polyesters such as poly(lactic acid), poly(ε-caprolactone), poly(-glycolic acid) and poly(glycerol sebacate), have been widely studied for the therapeutic devices including scaffolds for tissue engineering and drug carriers [3,4]. Since the first report of poly(glycerol sebacate) [PGS] by Langer group [5], extensive attention has been attracted to examine and improve the bioapplication of this interesting elastomer for clinical application. PGS is a highly interesting polymer because of its flexibility, for example, degradation rate can be tailored by controlling the degree of cross-linking, structure and morphology [6,7]. More importantly, PGS has proven less inflammation than another widely used biopolymer, poly(lactic-*co*-glycolic acid), probably because of the non-toxic reactants [8].

Although PGS has such advantages, as a synthetic polymer, its biocompatibility is still an issue which is the bottleneck of the biopolymer. One of the major drawbacks of PGS is cytotoxicity caused by fast degraded sebacic acid [7]. The cytotoxicity of the PGS strongly relies on its degradation rate, the carboxylic acids produced by aqueous hydrolysis of the PGS and this decreases the local extracellular pH value to below physiological values [7]. The increment in the acidity of the surrounding environment can easily provoke cell death. Therefore, many studies have been performed to improve the biocompatibility of PGS which is challenging as determined by a group of factors, for example, degradation rate, surface hydrophilicity, degree of cross-linking and swelling effect.

* Corresponding author.
E-mail address: junwang.tang@ucl.ac.uk (J. Tang).

https://doi.org/10.1016/j.mtadv.2019.100023

Adding particles such as bioglass [9], silica [10,11], or cellulose [12] in the polymer matrix was proved to increase the degree of cross-linking and reduce the degradation rate but not all four factors, which would dominate cell viability on a polymer matrix.

As mentioned above, the surface state of a polymer plays a critical role in its bioapplication, which can affect the cell proliferation. Specifically, polymer's biological performance can be enhanced by changing its surface topographical (i.e. roughness) or chemical/physical characteristics (i.e. hydrophilicity) [13]. PGS surface could be hydrophobic or hydrophilic which depends on the experimental conditions. When increasing the molar ratio of sebacic acid to glycerol, the surface becomes more hydrophobic, probably because of the reduced amount of hydroxyl backbone which reacts with carboxylic acids to form the ester linkage [14,15]. Therefore, there is a dilemma between a hydrophilic surface and a high degree of cross-linking, and both are highly desirable for a biopolymer.

On the other hand, calcium phosphate ceramics are generally used to improve the biocompatibility of other biomaterials by coating a layer of calcium phosphate on the surface of bioinert or bioactive materials because they offer low toxicity, excellent biocompatibility and osteoconductivity [16]. Among these calcium phosphates, β-tricalcium phosphate (β-TCP) is more attractive because of its high biocompatibility, biological safety, ease of sterilization and long shelf life [17]. More importantly, β-TCP has proven its osteogenic properties preclinically [18].

Given advantages of both PGS and β-TCP, PGS has been modified with β-TCP particles by *in situ* microwave synthesis approach herein, which has recently shown a great potential to synthesize materials because of its fast reaction rate, high reproducibility, improved product selectivity and yields [19–21]. Such biocomposites alter the morphology, degree of cross-linking and hydrophilicity of PGS, leading to a dramatically enhanced biocompatibility. The prepared samples were also investigated in cell viability, which further proves the advance of the new biocomposite.

2. Material and methods

2.1. Synthesis of poly(glycerol sebacate)/β-tricalcium phosphate biocomposite

PGS was synthesized using the method recently developed by us [22]. Equimolar of glycerol (99%, Sigma Aldrich) and sebacic acid (>99%, Sigma-Aldrich) were mixed in a round bottom flask and heated in Discover SP microwave for 12 min (4 × 3 min per cycle) under nitrogen gas. A cooling interval was introduced after each cycle to minimize the overheating of monomers and increase the microwave efficiency. The prepolymer was then cured in vacuum oven at 120 °C for 8 h.

On the other hand, the synthesis of β-TCP followed our previous procedures [23]; 0.79 g of calcium acetate monohydrate (≥99%, Sigma Aldrich) and 0.33 g of phosphoric acid (≥98%, Acros Organics) were weighed and dissolved each in 20 mL of methanol (≥99.8%, Sigma-Aldrich). The acid solution was added drop-wisely into the calcium solution and then transferred to a sealed polytetrafluoroethylene (PTFE) vessel. The reaction mixture was then ramped for 25 min to preset temperature for a certain time. The produced powders were washed with deionized water and dried in the oven overnight.

For biocomposite fabrication, the prepared PGS was added into the vessel and then the precursor solution of β-TCP was added, followed by the irradiation with stirring in a microwave cavity (MARS, CEM Company). Similar to the previous preparation, the reaction mixture was ramped for 25 min to the preset temperature ranging from 120 to 180 °C and held for 5–60 min, where 60 min was required for all temperatures except 180 °C at which only 5 min was needed. PGS/β-TCP biocomposites were then removed from the vessel and washed with deionized water several times. Finally, the biocomposite was dried in the drying oven at 60 °C overnight, denoted as PGS/β-TCP120, PGS/β-TCP150 and PGS/β-TCP180, depending on the reaction temperature.

2.2. Characterization methods

The synthesized calcium phosphate particles by microwave approach at different temperature were identified using Powder X-ray Diffractometer (Bruker D8 Advance Diffractometer, Bruker, UK) with a CuK_{α} ($\lambda = 0.1541784$ nm) radiation source. Diffraction patterns were collected from 10° to 80° and a maximum step size of 0.05° with 5 s per step was applied. These diffraction patterns were compared with the standard spectra from the joint committee on powder diffraction standards (JCPDS) database. The functional groups of the prepared PGS/β-TCP biocomposites were confirmed using a PerkinElmer 1605 FTIR spectrometer in attenuated total reflection (ATR-FTIR) mode with a wavenumber range of 400–4000 cm^{-1} at 4 cm^{-1} resolution. Raman spectra data of the synthesized PGS/β-TCP biocomposites were acquired using a Renishaw Raman microscope with a helium-neon laser at a wavelength of 514.5 nm and 10 scan numbers. Thermal gravimetric analysis (TGA) was conducted by a PerkinElmer Pyris 1 TGA analyzer. Approximately 5 mg of samples were used for the tests, the heating programs were set from 50 to 800 °C with ramping of 10 °C/min, sample temperatures were collected from room temperature. To observe the morphology of prepared PGS/β-TCP biocomposite, SEM (XL 30, Philips, Eindhoven, Netherlands) was operated at 5–10 kV and a working distance of 10 mm. Owing to low conductivity of the samples, a layer of Au was coated on the surface of the samples before SEM observation.

2.3. Sol/gel content analysis

The degree of cross-linking of the specimens was determined by sol (non-cross-linked network) and gel (cross-linked network) content analysis which followed the reported method [10]. Biocomposite or PGS was weighed (W_i) and then submerged in tetrahydrofuran (THF) for 24 h. The swollen samples were dried overnight and the final weight (W_f) was measured. The percentage of sol and gel content (%) was calculated using Eqs. (1) and (2):

$$Sol\ (\%) = \frac{W_i - W_f}{W_i}\ x100\% \tag{1}$$

$$Gel\ (\%) = 100\% - Sol(\%) \tag{2}$$

where W_i is the initial weight of the specimens and W_f is the residual mass of the specimens at the preset time.

2.4. Hydration

Hydration properties of samples were evaluated from swelling ratio and contact angle measurement. For the swelling study, samples were weighed (W_i) and then submerged in phosphate buffer saline (PBS) at 37 °C for 48 h. The excess water was drained and the weight of the swollen sample (W_s) was measured. The swelling ratio was calculated using Eq. (3):

$$Swelling\ ratio = \frac{W_s}{W_i} \tag{3}$$

Surface hydrophilicity was determined by water contact angle analysis. The contact angle measurements of the samples were obtained with a goniometer (Cam 200, KSV Instruments Ltd). A drop of 10 μL size of water was dripped onto the biocomposite surface. The mean value of the contact angles was calculated by the Cam2008 software (KSV Instruments Ltd) on three specimens.

2.5. Degradation and cell culture

Five or more specimens with a dimension of 5 × 5 mm^2 were stored in the standard PBS, 1 X at 37 °C. The samples were collected after 7, 14, 21 and 28 days and then dried in an oven at 60 °C overnight. The percentage of mass loss (%) was calculated using Eq. (4):

$$Mass\ loss\ (\%) = \frac{W_{initial} - W_{final}}{W_{initial}}\ x100\% \quad (4)$$

where $W_{initial}$ is the initial weight of the biocomposites or PGS and W_{final} is the residual mass of the biocomposites or PGS at the preset time.

Human Mesenchymal Stem Cells (hMSCs) (passage 3) were used for this cell culture studies. Initially, cells were incubated for growing at standard condition (37 °C, 95% air, 5% CO_2, 95% relative humidity) in Dulbecco's Modified Eagle Medium (DMEM, Gibco, Life Technologies, Paisley, UK) supplemented with 10% fetal bovine serum (Gibco) and 1% penicillin/streptomycin (PAA Laboratories, GE Healthcare, Chalfont St. Giles, UK). When cell confluency percentage reached 80%, they were trypsinized and ready for seeding on the prepared samples. PGS and its biocomposites were sterilized by UV light exposure for 20 min on both sides before the seeding process.

A triplicate of specimens was used for this study. hMSCs were initially seeded at density of 15000 cells/polymer in 24-well plates. Seeding was undertaken by pipetting out the intended cell density in 10 μL of culture media on the polymer to ensure cells did not flow away from the sample. Then they were kept in the incubator for 1 h to ensure cell attachment on the polymers. 1 mL of culture media was added to each polymer. Culture media was changed every three days.

A cell-count kit (CCK) assay was carried out in three time points (day 1, 4 and 7). At each time point, 10% of the assay reagent was added to the sample and incubated for 1 h. Subsequently, a fluorescence measurement was taken for each well plate and this measurement was repeated three times by using wavelength detector (Infinite® M200, Tecan) at 450 nm wavelength.

Glass discs cover slips were used in a control experiment. A calibration curve was obtained by seeding the cells in predetermined five different cell densities and fluorescence was measured for each cell density. Fluorescence absorbance was correlated with cell number which generated a calibration curve and an equation that was accordingly used for indirect cell counting. Cell culture data were statistically analyzed by SPSS software by using Kruskal-Wallis analysis where *p*-value for statistical significance was ≤ 0.05.

3. Results and discussion

3.1. Synthesis of PGS/β-TCP biocomposites

Calcium phosphate particles prepared by microwave at different reaction temperatures and times were characterized by X-ray diffraction (XRD) spectroscopy, as illustrated in Fig. 1a. The phase of the synthesized calcium phosphate matches with the standard diffraction pattern of β-TCP (JCPDS #09–0169) [24]. The phase of the calcium phosphates does not alter with the reaction temperature and reaction time in the microwave. This is because the formation of β-TCP relies on the solvent species in which the solubility of both calcium and phosphate precursors affects the final phase of the calcium phosphates [23]. The characteristic peaks associated with β-TCP in literature were reported at a few regions: symmetric P–O stretching vibrations (ν_1:960 cm^{-1}), antisymmetric P–O bending vibrations (ν_4: 650-400 cm^{-1}), and antisymmetric P–O stretching vibration (ν_3: 1010-1090 cm^{-1}) [25,26]. From the Raman spectra of β-TCP(Fig. 1b), the peaks are also comparable with the literature, showing the symmetric P–O bending (ν_2), antisymmetric P–O bending (ν_4) and symmetric P–O bending (ν_1) around 400-460 cm^{-1}, 560-610 cm^{-1} and 950-970 cm^{-1}, respectively [26].

For PGS, ATR-FTIR analysis (Fig. 1c) was used to confirm the formation of ester bonds, indicated by an intense peak at 1735 cm^{-1}. The two absorption peaks around 2928 and 2855 cm^{-1} are attributed to the methylene group and the broad peak observed around 3400-3600 cm^{-1} is because of hydrogen bonded hydroxyl groups [9]. For the Raman spectra of PGS, there are no significant peaks found at the range between 200 and 1000 cm^{-1}(Fig. 1b).

The prepared biocomposites (i.e. PGS/β-TCP120, PGS/β-TCP150 and PGS/β-TCP180) were then characterized by Raman (Fig. 1b) and ATR-FTIR (Fig. 1c) spectroscopy. Similar to PGS, ester linkage at 1735 cm^{-1}, methylene group at 2928 and 2855 cm^{-1}, and broad hydroxyl group at around 3400- 3600 cm^{-1} are observed in ATR-FTIR spectrum. Additional peaks corresponded to the P–O bond of the β-TCP are also found in these biocomposites. As illustrated in Fig. 1b, the Raman spectra of the PGS/β-TCP biocomposites show the peaks around 400-460 cm^{-1}, 560-610 cm^{-1} and 950-970 cm^{-1}, which correspond to symmetric P–O bending (ν_2), anti-symmetric P–O bending (ν_4) and symmetric P–O bending (ν_1), respectively [26]. Both infrared and Raman spectra thus prove that the β-TCP particles are incorporated with PGS.

SEM images of the PGS and its biocomposites (Fig. 2 as well as Figs. S1 and S2) reveal the spherical β-TCP particles with a dimension of 50–190 nm are well incorporated into PGS. The surface condition of the biocomposites also changes significantly when compared with PGS. The surface of PGS is generally smooth and the presence of β-TCP particles in the polymer results in an uneven/rough surface as illustrated in Fig. S1. Furthermore, higher temperature allows more particles to be attached in the PGS. PGS/β-TCP prepared at low temperature (120 °C) has less β-TCP particles that agglomerate on its surface. On the other hand, PGS/β-TCP150 and PGS/β-TCP180 biocomposites have much better incorporation of the β-TCP particles into PGS (Fig. 2 and Supporting information, Fig. S2). However, when comparing PGS/β-TCP150 and PGS/β-TCP180 biocomposites, β-TCP particles tend to agglomerate in the PGS polymer when the temperature is higher than 150 °C. PGS/β-TCP150 demonstrates a more homogeneous layer of β-TCP particles incorporated on the surface of the biocomposite. Furthermore, TGA as shown in Fig. 1d presents the mass ratios between PGS and β-TCP. PGS/β-TCP180 contains over 60 wt% of the original weight (namely the weight percentage of β-TCP is >60%), which is three times higher than PGS/β-TCP150. PGS/β-TCP120 has a slight larger weight loss than PGS/β-TCP150 although PGS losses 100% weight at 490 °C. Both the cross-section and surface images of the biocomposites in Fig. S2 in supporting information show β-TCP particles are well incorporated in the PGS matrix. Further energy dispersive X-ray spectroscopy (EDS) analysis in Fig. S3 in supporting information also presents the biocomposites are embodied by β-TCP particles. The figure also indicates more β-TCP particles on the surface of PGS/β-TCP150 than PGS/β-TCP180. Taking into account the results of TGA measurement, one can conclude that more β-TCP particles are incorporated into the bulk of PGS polymer when synthesized at 180 °C.

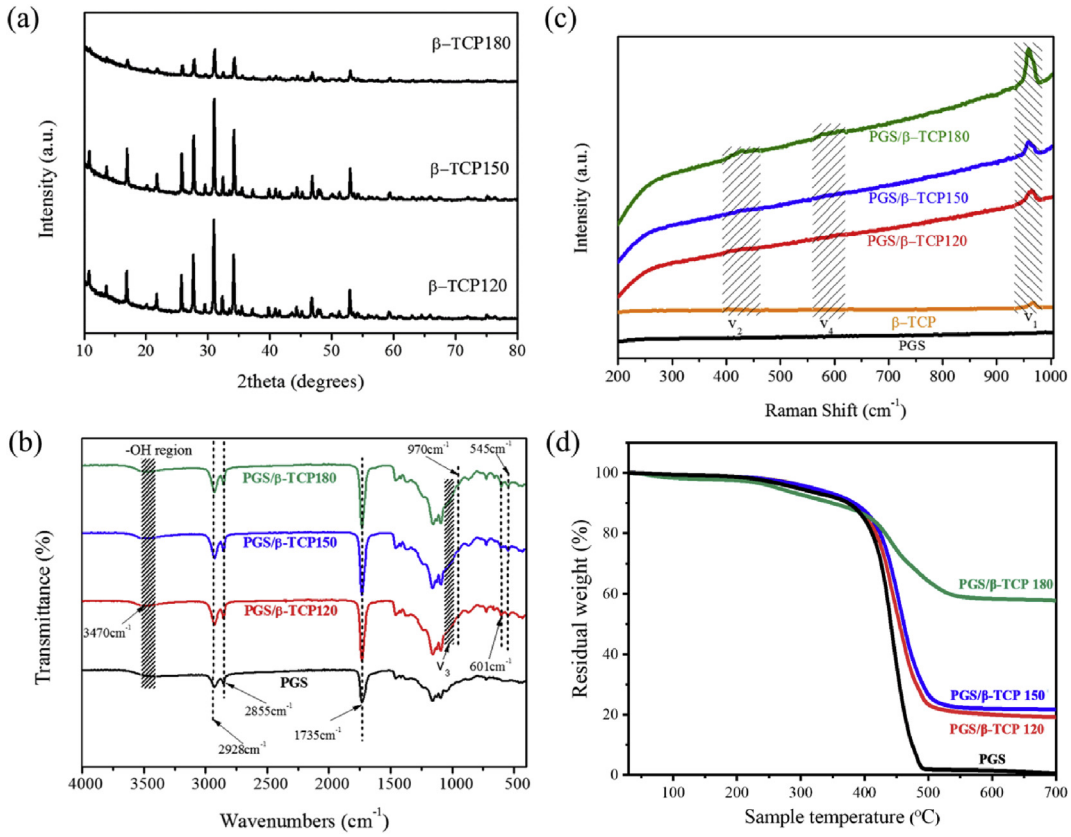

Fig. 1. **(a)** XRD of β-TCP particles prepared at different reaction temperatures and reaction time, where the reaction time is 60 min at 120 °C and 150 °C, although only 5 min at 180 °C. **(b)** Raman spectra of PGS/β-TCP biocomposite synthesized at 120 °C (60 min), 150 °C (60 min) 180 °C (5 min) by microwave, comparing with pure phase of PGS and β-TCP. **(c)** IR spectra of the prepared PGS/β-TCP biocomposites and pure PGS (d) TGA tests of the PGS/β-TCP biocomposites and the PGS polymer. PGS, poly(glycerol sebacate); β-TCP, β-tricalcium phosphate; IR, infrared; XRD, x-ray diffraction; TGA,thermal gravimetric analysis.

Based on the XRD patterns, IR spectra, Raman spectra and SEM images, the biocomposites of PGS/β-TCP were prepared successfully, where the presence of these β-TCP particles alters the morphology and surface conditions of the PGS. These altered surfaces would have different surface properties, changing their biocompatibility.

3.2. Improved surface properties/hydrophilicity

As mentioned above, the surface hydrophilicity of a biomaterial is crucial to cell adhesion and proliferation. Therefore, the surface of the biocomposites was investigated by measuring the swelling ratio and contact angle. Fig. 3 illustrates the swelling data for the PGS and its biocomposites. The swelling ratio of PGS/β-TCP150 increases by 8% to 1.16 ± 0.03 as compared with PGS which is only 1.07 ± 0.01 and followed by PGS/β-TCP180 which is 1.14 ± 0.01. PGS/β-TCP120 has comparable swelling ratio with PGS, also proving the lower incorporation of β-TCP particles in the PGS as seen in its SEM image (Supporting information, Fig. S1). The incorporation of β-TCP particles stimulates the water uptake owing to the changes in the surface. The uneven surface increases surface area-to-volume ratios of the biocomposites, and this also increases the amount of the absorbed water, which can affect the degradation rate [27]. Moreover, for PGS/β-TCP180, the agglomeration of β-TCP particles reduces the surface area-to-volume ratio, leading to lower swelling ratio when compared with PGS/β-TCP150.

The contact angle of these specimens was also examined. As shown in Table 1, the contact angle of the PGS implies that the PGS surface appears to be hydrophilic to some extent. PGS/β-TCP150 and PGS/β-TCP180 exhibit 14% lower contact angle than PGS (76.70 ± 2.30°), indicating these biocomposites have a better hydrophilic surface. On the other hand, PGS/β-TCP120 has a comparable contact angle to PGS because of two separate phases instead of a composite. The adding of the particles in the polymer generally affects both the degree of cross-linking and the hydrophilicity of the PGS. In this study, the incorporation of β-TCP particles improves the hydrophilicity because these particles are hydrophilic [28,29]. These β-TCP particles can interact with water, like the hydroxyl backbone of PGS and creating a hydrophilic surface, which is in agreement with a previous study [30]. On the other hand, the changes in the contact angle can be explained by Wenzel's equation: a larger surface area or a rough surface can reduce the contact angle of a hydrophilic surface because it increases the polar interaction with water droplets, leading to a lower contact angle [31,32]. These properties could affect the degradation kinetics and cellular responses as water molecules at the interfaces affect cell adhesion and proliferation [10].

3.3. Enhanced degree of cross-linking

Other than the surface properties, the degree of cross-linking of bulk materials was determined via sol-gel content. Theoretically, the cross-linked part swells and the non-cross-linked part leaches out from the polymer in THF solution. Therefore, the remaining dry weight of the cross-linked network is used to determine the gel content of the biocomposite network. Fig. 4 shows that sol content (non-cross-linked monomer) decreases when incorporating the β-TCP particles into PGS. For instance, the sol content of PGS/β-

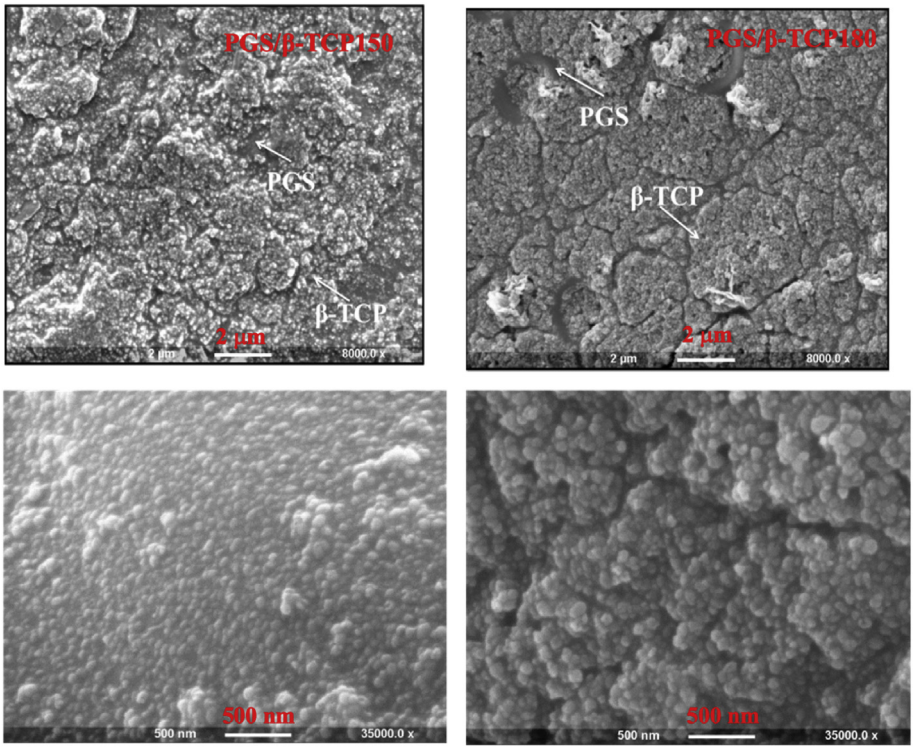

Fig. 2. SEM images of PGS/β-TCP150 (left) and PGS/β-TCP180 (right) biocomposite with different magnification. The agglomeration of β-TCP particles is observed for PGS/β-TCP180 although PGS/β-TCP150 has a more homogeneous distribution of these particles. PGS, poly(glycerol sebacate; β-TCP, β-tricalcium phosphate.

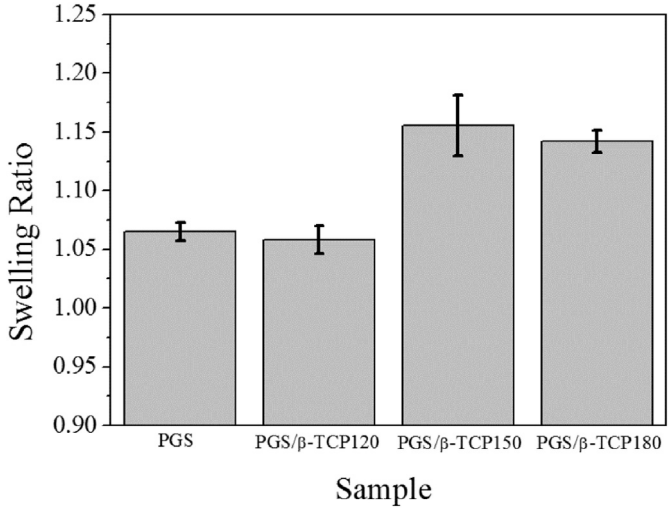

Fig. 3. Swelling ratio of the PGS and its biocomposites at different reaction temperature and time in the microwave.

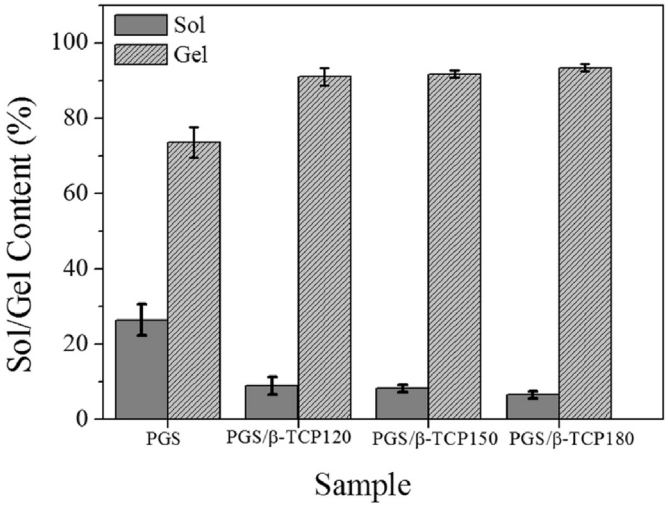

Fig. 4. Effects of β-TCP particles on degree of cross-linking is determined by the sol-gel content. The presence of β-TCP particles dramatically reduces the sol (non-cross-linked) and increases the gel (cross-linked) content.

Table 1
Contact angle of the PGS and its biocomposites prepared at different reaction temperature and time in microwave

Sample	Contact angle (°)
PGS	76.70 ± 2.30
PGS/β-TCP120	72.95 ± 9.80
PGS/β-TCP150	65.65 ± 7.34
PGS/β-TCP180	65.95 ± 4.11

PGS, poly(glycerol sebacate; β-TCP, β-tricalcium phosphate.

TCP150 biocomposites decreases by at least 66% as compared with PGS sample, which is 26.43 ± 4.10%. All the biocomposites show a higher degree of cross-linking where the sol content is only 8.93 ± 2.35%, 8.25 ± 0.98% and 6.59 ± 0.97% for the PGS/β-TCP120, PGS/β-TCP150 and PGS/β-TCP180, respectively. Although an increase in synthesis temperature of biocomposite is likely to result in a further cross-linking of unreacted carboxylic site (-COOH) and (-OH) on the cured PGS prepared at 120 °C for 8 h, the comparable percentage sol contents after 120, 150 and 180 °C microwave heating suggest that the effect of biocomposite synthesis

temperature to the cross-linking is insignificant. Thus, the reduction in the sol content of prepared biocomposites is attributed in the incorporation of β-TCP particles in the polymer matrix which increases the degree of cross-linking [9–11]. This may be due to the electrostatic interaction between 'Ca^{2+} site bridging' mechanisms, that is, negatively charged of unreacted carboxylic site ($-COO^-$) or the unreacted ($-OH^-$) presented on the PGS binds to Ca^{2+} of β-TCP [9].

Degradation properties of biomaterials have significant effects on their application in tissue engineering as it should match with the rate of new tissue regeneration. Under physiological conditions, PGS degrades due to surface erosion via cleaving the ester linkage. The surface erosion is advantageous over bulk degradation because this type of erosion exhibits gradual loss in geometry in relation to mass loss.

Degradation of the PGS and PGS/β-TCP biocomposites were investigated under physiological conditions (PBS, 37 °C) for 4 weeks (Fig. 5). From the results, apparently, the mass loss of the biocomposites reduces significantly when compared with PGS. After 7 days, the mass loss of PGS is the highest which is 8.84 ± 0.94% and maximum 3% for the biocomposites. Similar trend is observed after 28 days where the residual mass of PGS is less than 83% compared with all biocomposites (>92%), indicating the biocomposites have a ca. 10% slower degradation rate. On the other hand, the morphology of these degraded samples after 28 days was observed using SEM to examine the effect of degradation on their surface morphology. The images show that many evenly distributed β-TCP particles are still found on the surface of biocomposites, especially for those two prepared at a higher temperature (i.e. PGS/β-TCP150 and PGS/β-TCP180) as shown in Supporting information, Fig. S4, indicating such biocomposites undergo the same surface erosion mechanism which is mainly dominated by hydrolysis of PGS, and these β-TCP particles are relatively incorporated into the polymer matrix.

The degradation rate of the biocomposites is slower than PGS owing to a higher degree of cross-linking as observed by the sol/gel analysis. Increase in the gel content indicates a higher degree of cross-linking, and the degradation rate is always inversely proportional to the degree of cross-linking. Therefore, PGS with the highest sol content degrades faster than the biocomposites. This is because the incorporation of β-TCP particles into PGS can retard the degradation of the polyester backbone and enhance physiological stability by increasing the degree of cross-linking. Furthermore, swelling ratio also plays a critical role in the degradation rate. Higher swelling ratio allows more water to be absorbed and results in a faster degradation rate [27]. Therefore, PGS/β-TCP150 with the highest swelling ratio shows the fastest mass loss among these biocomposites.

The short-term degradation of these biocomposites is mainly dominated by the hydrolysis of PGS, but long term degradation is complex and requires further investigation which involves the degradation of the β-TCP particles where β-TCP is a weak water soluble inorganic salt and it could be dissolved slowly from the composite after a long period. For instance, only approximately 5% of TCP mass loss was observed from its composite after 15 weeks [10,33].

3.4. In vitro bioactivity

After investigating the properties of the biocomposites, PGS/β-TCP150 and PGS/β-TCP180 were selected to study their biocompatibility owing to their improved hydrophilicity and reduced degradation rate. Fig. 6 presents cell proliferation data over three intervals (at day 1, 4, and 7). Initially cells were seeded at a density of 15000 cells/biocomposite. Overall, there is a continuous cellular growth over time in all samples. At day 1, the control sample (glass discs) exhibits the highest proliferation rate at around 27800 ± 2400 cells, being statistically different from the PGS samples (the statistic value *p* shows the significant differences between samples when it is less than 0.05). The cell numbers in both PGS/β-TCP150 and PGS/β-TCP180 are approximately 16500–18000 cells each biocomposite as compared with the PGS samples that are less than 10000 cells per sample, and is in agreement with the previous study [9]. Both of the biocomposites increase 65% of cell proliferation rate when compared with PGS. At day 4, a similar trend is found where the highest cellular proliferation is noticed in the control experiment (on a glass discs), followed by the PGS/β-TCP (around 26000–26400 cells each biocomposite) and the least growth is observed in the PGS samples which is only 18795 ± 561 cells per sample. This further shows that the biocomposites show a 40% difference when compared with the PGS although they have a similar surface area where cells

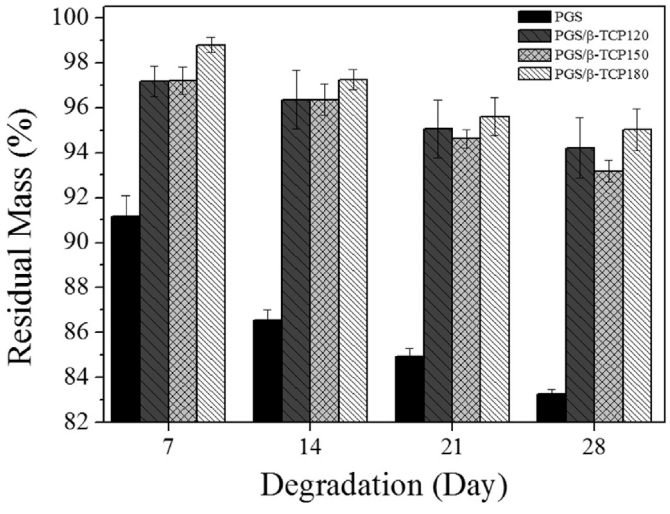

Fig. 5. Degradation rates of the PGS and PGS/β-TCP biocomposites at day 7, 14, 21, and 28.

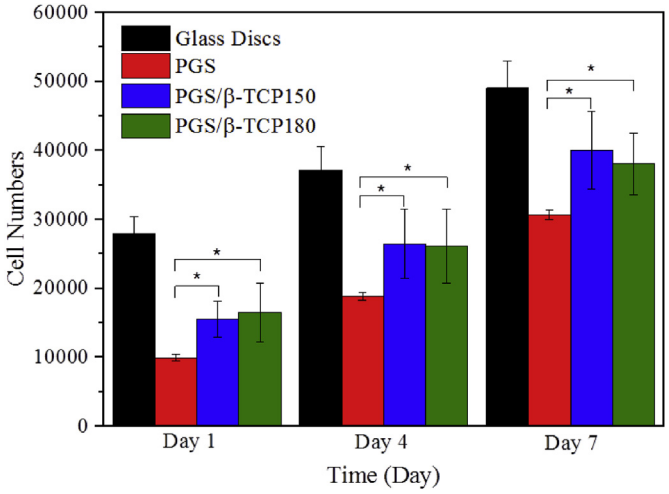

Fig. 6. Cell viability study of the PGS and PGS/β-TCP biocomposites with the control glass discs where the measurements were taken at day 1, 4 and 7. The two selected biocomposites do not show the significant difference between each other ($p > 0.05$), but the PGS and the biocomposites exhibits significant difference in cell viability ($p < 0.05$). *$p < 0.05$.

proliferation takes place. At day 7, cell proliferation figures of all the samples are about double of that on day 1. Both PGS/β-TCP150 and PGS/β-TCP180 still illustrate higher proliferation rate than PGS samples, which is at least 24% increase in cell viability than PGS sample (30637 ± 722 cells per sample). The findings of this study show that the cell number in both PGS/β-TCP150 and PGS/β-TCP180 increases in a similar rate, although a better cell viability than PGS ($p < 0.05$). Therefore, this can summarize that the biocomposites are more biocompatible than PGS for cell viability in particular for a short-time proliferation, which better matches with the bone growth when using in implants.

The bioactivity studies display the biocomposites show promising results where both biocomposites showing significant difference in cell number when compared with the PGS. This can be interpreted by relating the biocomposite degradation rate with cell bioactivities. First, a slower degradation rate may provoke cellular metabolic and proliferative activities. In other words, the cell viability is inversely related to the degradation rate [10,34,35]. The sebacic acids degraded from the hydrolysis process of PGS could lower the local pH and produce an acidic environment which is unfavorable for the cell viability [9,36]. Second, the hydrophilic surface and better swelling effect are preferable for cell proliferation as proved in the reported literatures [37–39], therefore the improved hydrophilic surface of biocomposites shows a better cell viability. Third, as compared with a single polymer material, the presence of β-TCP particles can improve the cell viability and proliferation owing to its biocompatibility and non-toxicity. In addition, as suggested by Hu et al. [40] the high crystallinity of the β-TCP can also affect the cell proliferation. As such the PGS/β-TCP150 and PGS/β-TCP180 show the improved cell viability after 7 days among these biomaterials because of slower degradation rate, smallest contact angle and largest swelling effect.

It can be summarized that the incorporation of β-TCP particles not only reduces the degradation rate but also improves the surface hydrophilicity and swelling effect. The improved properties dramatically enhance the biocompatibility of PGS which could not be achieved by a single PGS biomaterial. This is because the hydrophilicity and degree of cross-linking of PGS always conflict with each other. For instance, to decrease the degradation rate, the degree of cross-linking of PGS needs to be increased, while this reduces the free hydroxyl bonds in the backbone of PGS and then affects the hydrophilicity of the polymer, although it is beneficial for cell proliferation. Another benefit of composing β-TCP into a polymer is to promote the new bone ingrowth and to buffer the drop in pH during the degradation process, as suggested by Roy et al. [41]. This is because β-TCP particles can resorb and induce cell proliferation which is beneficial for new bone formation and is hardly to be achieved by PGS [42].

4. Conclusion

In this work, we successfully *in situ* fabricated PGS/β-TCP biocomposites by a fast microwave synthesis approach. The degree of cross-linking, hydrophilicity, and morphology of the biocomposites have been altered with the presence of these biocompatible β-TCP particles with a size of 50–190 nm. Specifically, these β-TCP particles improved the degree of cross-linking by decreasing the sol content by ca. 66% and enhanced the hydrophilicity as indicated by the smaller contact angle. Such biocomposites also increased the swelling ratio of the biopolymer by nearly 10%. The degradation rate of these biocomposites also changed notably, decreasing more than two times after 28 days in the PBS solution compared with pure PGS polymer. Many β-TCP particles were observed after 28 days degradation test, indicating these β-TCP particles were relatively evenly incorporated into the polymer matrix. As a result, the biocomposites (i.e. PGS/β-TCP150 and PGS/β-TCP180) proved higher cell viability, for example,. after one day, the optimized biocomposites increased cell viability by at least 65% compared with pure PGS polymer. It can be concluded that a slower degradation rate (higher degree of cross-linking), better hydrophilic surface, and higher swelling effect support the attachment and proliferation of cells, resulting in the best biocompatibility of the new biocomposites prepared by the fast and facile microwave approach, which would meet the requirement of a drug carrier or an implant.

Declaration of competing interest

The authors declare that they have no known competing financial interests or personal relationships that could have appeared to influence the work reported in this paper.

Acknowledgments

All authors would like to thank Ms Yiting He for conducting the TGA tests. J Tang acknowledges the funding from Royal Society Newton Advanced Fellowship grant (NA170422) and Leverhulme Trust (RPG-2017-122). CC Lau is supported by postgraduate scholarship from the Public Service Department of Malaysia. This research was partially funded by the European Commission Seventh Framework Programme under Grant agreement No. v739572.

Appendix A. Supplementary data

Supplementary data to this article can be found online at https://doi.org/10.1016/j.mtadv.2019.100023.

References

[1] S.M. Kurtz, J.N. Devine, PEEK biomaterials in trauma, orthopedic, and spinal implants, Biomaterials 28 (2007) 4845–4869, https://doi.org/10.1016/j.biomaterials.2007.07.013.
[2] R. Ma, T. Tang, Current strategies to improve the bioactivity of PEEK, Int. J. Mol. Sci. 15 (2014) 5426–5445, https://doi.org/10.3390/ijms15045426.
[3] L.S. Nair, C.T. Laurencin, Biodegradable polymers as biomaterials, Prog. Polym. Sci. 32 (2007) 762–798, https://doi.org/10.1016/j.progpolymsci.2007.05.017.
[4] R. Shi, D. Chen, Q. Liu, Y. Wu, X. Xu, L. Zhang, Recent advances in synthetic bioelastomers, Int. J. Mol. Sci. 10 (2009) 4223–4256, https://doi.org/10.3390/ijms10104223.
[5] Y. Wang, G. Ameer, B. Sheppard, R. Langer, A tough biodegradable elastomer, Nat. Biotechnol. 20 (2002) 602.
[6] Q. Chen, S. Liang, G.a. Thouas, Elastomeric biomaterials for tissue engineering, Prog. Polym. Sci. 38 (2013) 584–671, https://doi.org/10.1016/j.progpolymsci.2012.05.003.
[7] X.J. Loh, A.A. Karim, C. Owh, Poly(glycerol sebacate) biomaterial: synthesis and biomedical applications, J. Mater. Chem. B. 3 (2015) 7641–7652, https://doi.org/10.1039/C5TB01048A.
[8] C.A. Sundback, J.Y. Shyu, Y. Wang, W.C. Faquin, R.S. Langer, J.P. Vacanti, T.A. Hadlock, Biocompatibility analysis of poly(glycerol sebacate) as a nerve guide material, Biomaterials 26 (2005) 5454–5464, https://doi.org/10.1016/j.biomaterials.2005.02.004.
[9] S.L. Liang, W.D. Cook, G.a. Thouas, Q.Z. Chen, The mechanical characteristics and in vitro biocompatibility of poly(glycerol sebacate)-Bioglass® elastomeric composites, Biomaterials 31 (2010) 8516–8529, https://doi.org/10.1016/j.biomaterials.2010.07.105.
[10] P. Kerativitayanan, A.K. Gaharwar, Elastomeric and mechanically stiff nanocomposites from poly(glycerol sebacate) and bioactive nanosilicates, Acta Biomater. 26 (2015) 34–44, https://doi.org/10.1016/j.actbio.2015.08.025.
[11] X. Zhao, Y. Wu, Y. Du, X. Chen, B. Lei, Y. Xue, P.X. Ma, A highly bioactive and biodegradable poly(glycerol sebacate)– silica glass hybrid elastomer with tailored mechanical properties for bone tissue regeneration, J. Mater. Chem. B. 3 (2015) 3222–3233, https://doi.org/10.1039/C4TB01693A.
[12] L. Zhou, H. He, C. Jiang, S. He, Preparation and characterization of poly (glycerol sebacate)/cellulose nanocrystals elastomeric composites, J. Appl. Polym. Sci. 42196 (2015) 42196, https://doi.org/10.1002/app.42196.
[13] R. Bosco, J. Van Den Beucken, S. Leeuwenburgh, J. Jansen, Surface engineering for bone implants: a trend from passive to, Act. Surf. Coat. 2 (2012) 95–119, https://doi.org/10.3390/coatings2030095.

[14] Á. Conejero-garcía, H.R. Gimeno, Y.M. Sáez, G. Vilariño-feltrer, I. Ortuño-lizarán, A. Vallés-lluch, Correlating synthesis parameters with physicochemical properties of poly (glycerol sebacate), Eur. Polym. J. 87 (2017) 406–419, https://doi.org/10.1016/j.eurpolymj.2017.01.001.
[15] M.J. Kim, M.Y. Hwang, J. Kim, D.J. Chung, Biodegradable and elastomeric poly (glycerol sebacate) as a coating material for nitinol bare stent, BioMed Res. Int. (2014) 1–7.
[16] S.R. Paital, N.B. Dahotre, Calcium phosphate coatings for bio-implant applications : materials , performance factors , and methodologies, Mater. Sci. Eng. R. 66 (2009) 1–70, https://doi.org/10.1016/j.mser.2009.05.001.
[17] D. Le, L. Duval, A. Lecomte, M. Julien, J. Guicheux, G. Daculsi, P. Layrolle, Interactions of total bone marrow cells with increasing quantities of macroporous calcium phosphate ceramic granules, J. Mater. Sci. Mater. Med. 18 (2007) 1983–1990, https://doi.org/10.1007/s10856-007-3098-2.
[18] P. Gao, H. Zhang, Y. Liu, B. Fan, X. Li, X. Xiao, P. Lan, M. Li, L. Geng, D. Liu, Y. Yuan, Q. Lian, J. Lu, Z. Guo, Z. Wang, Beta-tricalcium phosphate granules improve osteogenesis in vitro and establish innovative osteo-regenerators for bone tissue engineering in vivo, Sci. Rep. 6 (2016) 1–14, https://doi.org/10.1038/srep23367.
[19] M.K. Bayazit, E. Cao, A. Gavriilidis, J. Tang, A microwave promoted continuous flow approach to self-assembled hierarchical hematite superstructures, Green Chem. 18 (2016) 3057–3065, https://doi.org/10.1039/C5GC02245B.
[20] D. Dallinger, C.O. Kappe, Microwave-Assisted synthesis in water as solvent, Chem. Rev. 107 (2007) 2563–2591.
[21] M.K. Bayazit, J. Yue, E. Cao, A. Gavriilidis, J. Tang, Controllable synthesis of gold nanoparticles in aqueous solution by microwave assisted flow chemistry, ACS Sustain. Chem. Eng. 4 (2016) 6435–6442, https://doi.org/10.1021/acssuschemeng.6b01149.
[22] C.C. Lau, M.K. Bayazit, J.C. Knowles, J. Tang, Tailoring degree of esterification and branching of poly(glycerol sebacate) by energy efficient microwave irradiation, Polym. Chem. 8 (2017) 3937–3947, https://doi.org/10.1039/C7PY00862G.
[23] C. Ching Lau, P.J.T. Reardon, J. Campbell Knowles, J. Tang, Phase-tunable calcium phosphate biomaterials synthesis and application in protein delivery, ACS Biomater. Sci. Eng. 1 (2015) 947–954, https://doi.org/10.1021/acsbiomaterials.5b00179.
[24] C. Zhou, X. Ye, Y. Fan, L. Ma, Y. Tan, F. Qing, X. Zhang, Biomimetic fabrication of a three-level hierarchical calcium phosphate/collagen/hydroxyapatite scaffold for bone tissue engineering, Biofabrication 6 (2014), 035013, https://doi.org/10.1088/1758-5082/6/3/035013.
[25] I.R. Gibson, I. Rehman, S.M. Best, W. Bonfield, Characterization of the transformation from calcium-deficient apatite to b -tricalcium phosphate, J. Mater. Sci. Med. 11 (2000) 533–539.
[26] R.G. Carrodeguas, S. De Aza, α-Tricalcium phosphate: synthesis, properties and biomedical applications, Acta Biomater. 7 (2011) 3536–3546, https://doi.org/10.1016/j.actbio.2011.06.019.
[27] J. Huang, E. Ten, G. Liu, M. Finzen, W. Yu, J.S. Lee, E. Saiz, A.P. Tomsia, Biocomposites of pHEME with HA/b-TCP (60/40) for tissue engineering: swelling , hydrolytic degradation , and in vitro behavior, Polymer (Guildf) 54 (2013) 1197–1207, https://doi.org/10.1016/j.polymer.2012.12.045.
[28] D. Petta, G. Fussell, L. Hughes, D.D. Buechter, C.M. Sprecher, M. Alini, D. Eglin, M.D. Este, Calcium phosphate/thermoresponsive hyaluronan hydrogel composite delivering hydrophilic and hydrophobic drugs, J. Orthop. Transl. 5 (2016) 57–68, https://doi.org/10.1016/j.jot.2015.11.001.
[29] M. Kester, Y. Heakal, A. Sharma, G.P. Robertson, T.T. Morgan, E.I. Altinogly, A. Tabakovic, M.R. Parette, S. Rouse, V. Ruiz-Velasco, J.H. Adair, Calcium phosphate nanocomposite particles for in vitro imaging and encapsulated chemotherapeutic drug delivary to cancer cells, Nano Lett. 8 (2008) 4116–4121, https://doi.org/10.1021/nl802098g.Calcium.
[30] C. Park, E. Kyo, L.D. Tijing, A. Amarjargal, H. Raj, C. Sang, H. Kyong, Preparation and characterization of LA/PCL composite fi bers containing beta tricalcium phosphate (β -TCP) particles, Ceram. Int. 40 (2014) 5049–5054, https://doi.org/10.1016/j.ceramint.2013.10.016.
[31] T. Kobayashi, K. Shimizu, S. Konishi, Novel combination of hydrophilic/hydrophobic surface for large wettability difference and its application to liquid manipulation, Lab Chip 11 (2011) 639–644, https://doi.org/10.1039/c0lc00394h.
[32] R.N. Wenzel, Resistance of solid surfaces to wetting by water, Ind. Eng. Chem. 28 (1936) 988–994, https://doi.org/10.1021/ie50320a024.
[33] F. Yang, W. Cui, Z. Xiong, L. Liu, J. Bei, S. Wang, Poly (L , L -lactide- co -glycolide)/tricalcium phosphate composite scaffold and its various changes during degradation in vitro, Polym. Degrad. Stab. 91 (2006) 3065–3073, https://doi.org/10.1016/j.polymdegradstab.2006.08.008.
[34] H. Sung, C. Meredith, C. Johnson, Z.S. Galis, The effect of scaffold degradation rate on three-dimensional cell growth and angiogenesis, Biomaterials 25 (2004) 5735–5742, https://doi.org/10.1016/j.biomaterials.2004.01.066.
[35] J. Yi, F. Xiong, B. Li, H. Chen, Y. Yin, H. Dai, S. Li, Degradation characteristics , cell viability and host tissue responses of PDLLA-based scaffold with PRGD and b -TCP nanoparticles incorporation, Regen. Biomater. (2016) 159–166, https://doi.org/10.1093/rb/rbw017.
[36] Q.Z. Chen, H. Ishii, G.A. Thouas, A.R. Lyon, J.S. Wright, J.J. Blaker, W. Chrzanowski, A.R. Boccaccini, N.N. Ali, J.C. Knowles, S.E. Harding, An elastomeric patch derived from poly(glycerol sebacate) for delivery of embryonic stem cells to the heart, Biomaterials 31 (2010) 3885–3893, https://doi.org/10.1016/j.biomaterials.2010.01.108.
[37] C.H. Kim, M.S. Khil, H.Y. Kim, H.U. Lee, K.Y. Jahng, An improved hydrophilicity via electrospinning for enhanced cell attachment and proliferation, J. Biomed. Mater. Res. B Appl. Biomater. (2005) 283–290, https://doi.org/10.1002/jbmb.
[38] T. Gratiela, M. Daniela, R. Gabriela, D. Iordachescu, Effect of hydrophilic – hydrophobic balance on biocompatibility of poly (methyl methacrylate) (PMMA)– hydroxyapatite (HA) composites, Mater. Chem. Phys. 118 (2009) 265–269, https://doi.org/10.1016/j.matchemphys.2009.03.019.
[39] L. Ghasemi-mobarakeh, M.P. Prabhakaran, M. Morshed, Bio-functionalized PCL nano fi brous scaffolds for nerve tissue engineering, Mater. Sci. Eng. C 30 (2010) 1129–1136, https://doi.org/10.1016/j.msec.2010.06.004.
[40] Q. Hu, Z. Tan, Y. Liu, J. Tao, Y. Cai, M. Zhang, H. Pan, X. Xu, R. Tang, Effect of crystallinity of calcium phosphate nanoparticles on adhesion, proliferation, and differentiation of bone marrow mesenchymal stem cells, J. Mater. Chem. 17 (2007) 4690–4698, https://doi.org/10.1039/b710936a.
[41] T.D. Roy, J.L. Simon, J.L. Ricci, E.D. Rekow, V.P. Thompson, J.R. Parsons, Performance of degradable composite bone repair products made via three-dimensional fabrication techniques, J. Biomed. Mater. Res. A 66 (2003) 283–291.
[42] A. Neamat, A. Gawish, A.M. Gamal-Eldeen, β-Tricalcium phosphate promotes cell proliferation, osteogenesis and bone regeneration in intrabony defects in dogs, Arch. Oral Biol. 54 (2009) 1083–1090, https://doi.org/10.1016/j.archoralbio.2009.09.003.